2009 American Control Conference
Hyatt Regency Riverfront, St. Louis, MO, USA
June 10-12, 2009

Two Degree of Freedom Control for Nanopositioning Systems: Fundamental Limitations, Control Design, and Related Trade-offs

Chibum Lee and Srinivasa M. Salapaka

Abstract— **This paper studies and analyzes fundamental trade-offs between positioning resolution, tracking bandwidth and robustness to modeling uncertainties in two-degree-of-freedom (2DOF) control designs for nanopositioning systems. The analysis of these systems is done in optimal control setting with various architectural constraints imposed on the 2DOF framework. In terms of these trade-offs, our analysis shows that the primary role of feedback is providing robustness to the closed-loop device whereas the feedforward component is mainly effective in overcoming fundamental algebraic constraints that limit the feedback-only designs. This paper presents (1) an optimal prefilter model matching design for a system with an existing feedback controller and (2) a simultaneous feedforward and feedback control design in an optimal $\mathcal{H}_\infty$ mixed sensitivity framework. The experimental results on applying these controllers show a significant improvement, as high as 330% increase in bandwidth for similar robustness and resolution level over optimal feedback-only designs. Other performance objectives are similarly improved. We demonstrate that the 2DOF freedom design achieves performance specifications that are analytically *impossible* for the feedback-only design.**

I. Introduction

One of the pivotal requirements of nanotechnology is nanopositioning. Nanoscientific studies as well as applications, such as in scanning probe microscopy (SPM), demand positioning systems with atomic scale resolutions. There is an added impetus on design of nanopositioning systems since they form the bottleneck in terms of speed and accuracy of most devices for nano-investigation, especially in SPMs. For instance in atomic force microscopy (AFMs), the positioning resolution and tracking bandwidth of positioning systems is typically few orders less than the imaging resolution and bandwidth that microcantilever probe provides. Besides high precision positioning, most nanoscientific studies and applications impose severe demands on the tracking bandwidth and reliability in terms of repeatability of experiments. High tracking bandwidth is required as many studies, especially in biology and material science, require assaying matter with nanoscale precision over areas with characteristic lengths that are typically three orders or more. Repeatability of experiments is essential for validation of the underlying studies and this requirement translates to robustness of positioning systems to modeling uncertainties and operating conditions. Devices that are insensitive to (robust to) diverse operating conditions give repeatable measurements, and are hence reliable. The main challenges to design of robust broadband nanopositioning systems come from flexure-stage dynamics that limit the bandwidth of the positioning stage, difficult to model nonlinear effects due to piezoactuators such as hysteresis and creep, and sensor noise management issues in control feedback that can potentially hamper the tracking-resolution of the device.

There have been many efforts to counter these challenges which include design changes in the open-loop implementation such as: using 'harder' piezoceramics which have smaller nonlinear effects at the cost of travel range [1]; replacing voltage control by charge control [2] which achieves lower hysteresis but leads to more creep, lesser travel and lower positioning bandwidth; and compensating for the adverse nonlinear effects by a careful modeling of the nonlinearities, especially hysteresis, as in [3], [4], [5]. Recent work with feedback control designs have demonstrated that make positioning resolution practically independent of piezoelectric nonlinearities, where nonlinear effects become negligible compared to measurement noise. A feedback control framework presented in [6] determines and quantifies trade-offs between performance objectives, assesses if desired specifications are feasible and provides a way to design controllers to achieve specifications when possible. They have achieved substantial improvements in performance objectives of bandwidth, resolution as well as robustness to operating conditions and unmodeled dynamics [6], [7], [8]. More recently, 2DOF design schemes are being demonstrated for further improvements in nanopositioning systems. In [9], a 2DOF design is presented where the regular feedback control is appended with a feedforward scheme that exploits the information from previous scan line to improve scanning performance for imaging the current scan line. In [5], an optimal feedforward control design scheme that is integrated with the feedback design is discussed. In [10], [11], iterative learning schemes are used along with the feedback control to get improvements on the feedback-only design.

This paper presents 2DOF control design for nanopositioning systems in optimal control framework. The main contributions of this paper are threefold. First, it characterizes fundamental limitations on the space of achievable performance specifications as well as quantifies and analyzes the trade-offs between positioning-resolution, tracking bandwidth and robustness to modeling uncertainties in the 2DOF design scheme. More specifically, it discusses the extent of increase in the space of feasible performance specifications in the 2DOF design scheme when compared to the feedback-only design. Second, it poses optimization

This work was supported by NSF Grant Nos. ECS 0449310 CAR and CMMI 08-00863. C. Lee and S. Salapaka are with the Department of Mechanical Sciences and Engineering, University of Illinois, Urbana-Champaign, IL 61801, USA, contact email: salapaka@uiuc.edu

978-1-4244-4524-0/09/$25.00 ©2009 AACC

problems for determining *simultaneously* both the feedback and feedforward control laws to achieve design specifications, that are within the fundamental constraints. It presents the optimal 2DOF control design as well as its implementation for practical scenarios - when the feedback design is given a priori, and when neither feedback design is given nor the responsibilities-sharing given a priori. Third, it presents analysis and comparison of roles of feedforward and feedback components of 2DOF design, and studies the extent of improvements over the feedback-only designs and what limits them. Theoretical assertions are substantiated by experimental data. In particular, experimental results are provided that prove that 2DOF designs do achieve performance specifications which no feedback-only design can achieve.

II. Performance Objectives and Limitations

A typical nanopositioning system used in SPM is comprised of a flexure stage, actuators (typically piezoelectric) and/or sensors along with the feedback system. A schematic of a nanopositioning system is shown in Figure 1. Here, G represents the *scanner* that includes the actuators, flexure stage and sensors, r represents the tracking-reference signal, d represents the *mechanical noise*- the effects of unmodeled dynamics, n represents the sensor noise, $y_m = y + n$ represents the noisy measurement signal and K represents the control transfer function. The main objective for the design of the controller K is to make the *tracking error* small, that is to make the difference r-y between the desired and actual motions small. In open-loop positioning systems,

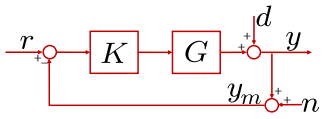

Fig. 1. A schematic of a nanopositioning system. The transfer function G represents the flexure stage along with the actuator and the sensor. The measured signal y_m represents the deflection y of the flexure stage along with the measurement (electronic) noise n. The signal d represents the mechanical noise (resulting due to unmodeled dynamics and operating conditions). The controller K is designed to make the signal y track the reference r.

the performance is severely limited by mechanical noise. The mechanical noise mainly consists of the slowly varying drift and creep, which are therefore prominent in slow scans, and the inertial lag at high frequencies, which is prominent in high speed scans. Hysteresis affects the systems at all frequencies and is particularly prominent in repetitive raster scanning. These nonlinear effects are sensitive to changes in operating conditions such as ambient temperature, residual polarization in piezoactuators, and most importantly the operating point, the reference value on the nonlinear input-output (input voltage versus stage displacement) graph about which stage motions are calibrated. Feedback based schemes (Figure 1) have demonstrated effective compensation for the creep, drift, hysteresis, and inertial lag problems without requiring their precise models [6]. They compensate for the mechanical noise but at the cost of feeding back the relatively smaller sensor noise. In this paper, we do not consider open-loop systems and analyze systems that have feedback along with feedforward components. We first present objectives and limitations in feedback-only designs and then present the 2DOF framework.

A. Performance Characterization and Control Objectives

The performance of a nanopositioning system is characterized by its positioning resolution, tracking bandwidth, and robustness to modeling uncertainties. For a given controller K, the tracking error in this configuration is given by

$$e = r - y = S(r - d) + Tn, \qquad (1)$$

where $S = (1 + GK)^{-1}$ and $T = 1 - S = (1 + GK)^{-1}GK$. Thus, low tracking error can be achieved by designing the feedback law K such that S and T are small in those frequency ranges where the frequency contents of r and n, respectively, are large. The resolution of the nanopositioning system is specified in terms of the standard deviation σ of the sensor output when there is no actuation of the positioning stage. The measurement noise typically exhibits a zero-mean Gaussian distribution. Thus, 3σ-resolution defined by the measurement noise gives over 99.7% confidence in any signal value that is greater than the resolution. The resolution of the closed-loop positioning system is determined by the term Tn and therefore lower values of T over larger ranges of frequencies guarantee better resolutions. More specifically, the standard deviation σ of the zero-mean position signal when reference signal is 0, which determines the resolution of the positioning system, is given by $\sigma = \int_0^\infty |T(j\omega)|^2 P_n(\omega) d\omega$, where $P_n(\omega)$ denotes the power spectral density of the noise signal n. Thus smaller the bandwidth of T, which is characterized by the roll-off frequency ω_T (Figure 2(a)), smaller the standard deviation σ, and hence better the resolution of the closed-loop device. The tracking bandwidth is characterized by the

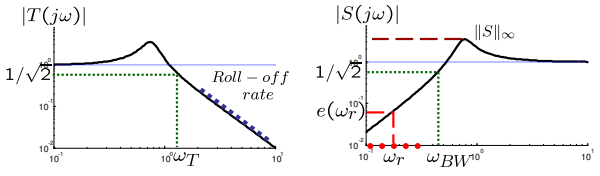

(a) (b)

Fig. 2. Objectives of feedback control. The objectives of the control design is to achieve high positioning resolution (by achieving low values ω_T, high roll-off rates in (a) and small error at reference frequencies $e(\omega_r)$ in (b)), high tracking bandwidth (by designing for large ω_{BW}) and robustness (by achieving $\|S\|_\infty$ close to 1).

corner frequency ω_{BW} as shown in Figure 2(b). We use the peak value of the magnitude of sensitivity function, $\|S\|_\infty$ to characterize the robustness of the system to modeling uncertainties and operating conditions (Figure 2(b)). Thus, the performance specifications translate to control design objectives of achieving high values of ω_{BW} for high tracking bandwidth, high roll-off rates of T and small values of ω_T for better positioning resolution, and low values of $\|S\|_\infty$ for better robustness to modeling uncertainties.

B. Limitations

These objectives have to be achieved under some practical and fundamental limitations. For instance, closed-loop bandwidth is limited by the sampling frequency allowed by the hardware and the feedback law is constrained such that the actuation signal should be within saturation limits of the hardware. The algebraic limitation $S+T=1$ prevents error $e=Sr-Sd+Tn$ from becoming small in all frequencies since S and T can not be made small simultaneously. Also, for scanner G with phase margin less than 90 deg which is true for most practical systems, the bandwidth ω_{BW} cannot be larger than ω_T[12]. This limitation prevents the feedback control to achieve noise attenuation over target reference frequency range. Another fundamental limitation that imposes a trade-off between the bandwidth, the resolution and the robustness requirements can be explained in terms of the Bode integral law $\int_0^\infty \log|S(j\omega)|d\omega = 0$ for stable system G with relative degrees of $KG \geq 2$. This shows a trade-off between the bandwidth and robustness to modeling uncertainties [12], [13].

Remark 1: The condition on the relative degree is typically satisfied for typical nanopositioning systems. Since T needs a sufficiently fast roll off rate at high frequencies for noise attenuation (and therefore better resolution), the open-loop transfer function $K(s)G(s)$ is designed such that it has greater than or equal to relative degree of order 2. Also when discrete system (or hybrid system-discrete control with analog system) is used, this relative degree condition is inherently satisfied [14]. ■

C. Two Degree of Freedom Control

Among various equivalent architectures for 2DOF control, we consider the scheme in Figure 3(a). The feedback-

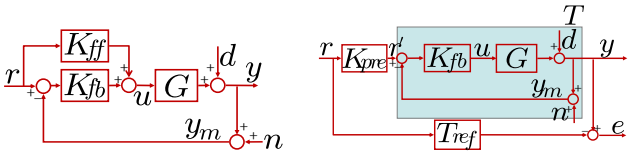

Fig. 3. (a) 2DOF control architectures. (b)Model matching prefilter problem

only control scheme is indeed a special case($K_{ff}=0$) of the 2DOF scheme. In this paper, we explore to what extent the performance becomes better. In 2DOF scheme, the robustness to modeling uncertainties as well as resolution of the device are determined only be the feedback part of the controller, that is the transfer function from d to y that characterizes robustness to modeling uncertainties is still determined by the sensitivity function S, and the transfer function from n to y that characterizes resolution is still determined by the complementary sensitivity function T. The main difference and advantage in 2DOF control design compared to the feedback-only design stems from the fact that the transfer functions from r to y and from n to y are different. This difference gives greater independence in designing for better trade-offs between different performance objectives. We use T_{ry} and S_{er} to denote the transfer function from r to y and from r to e, respectively, that is $S_{er}=S(1-GK_{ff})$, $T_{yr}=SG(K_{ff}+K_{fb})$. In this notation, the closed-loop transfer functions are given by

$$y = T_{yr}r - Tn + Sd,\ e = S_{er}r + Tn - Sd, \qquad (2)$$
$$u = S(K_{ff}+K_{fb})r - SK_{fb}n - SK_{fb}d.$$

The control objectives translate to small roll-off frequency as well as high roll-off rates for T to have good resolution, long range of frequencies for which S_{er} is small to achieve large bandwidth and low (near 1) values of the peak in the magnitude plot of $S(j\omega)$ for robustness to modeling uncertainties. Even though the 2DOF control design has greater flexibility than the feedback-only design, the main challenges to design still arise from practical and algebraic (albeit fewer) limitations. In the following, we show that the feasible space of performance specifications, which are constrained by the limitations described above in feedback-only configuration, can be extended by using a 2DOF design scheme.

III. 2DOF Control-Design Methods

A. Optimal Prefilter Model Matching Design

In some positioning systems, there is a pre-designed feedback component K_{fb} which cannot be replaced or changed (for instance, some commercial scanners come with feedback components designed to accomplish specific tasks such as raster scanning). However, typically, there are no such restrictions on the feedforward control design since it can be easily implemented as a prefilter on the reference signal. In the design presented here, the feedforward component K_{pre} is so chosen that the closed-loop positioning system mimics a *target* transfer function T_{ref} (Figure 3(b)), which satisfies desired performance objectives. An advantage of using such model matching schemes is that desired transient characteristics (such as settling times and overshoots) can be incorporated by choosing appropriate model T_{ref}. After noting that the closed-loop device transfer function from r to y is given by TK_{pre}, the feedforward component K_{pre} is chosen by solving an optimization problem such that the $\mathcal{H}_\infty$-norm of the mismatch transfer function $E=T_{ref}-TK_{pre}$ is minimized. Small values of $\|E\|_\infty$ guarantees small values for mismatch error signal given by $e=T_{ref}r-y=(T_{ref}-TK_{pre})r$. To ensure practical implementation, it is assumed that T_{ref} and T are stable proper transfer functions. This optimization problem is trivial if T is a minimum phase transfer function, that is if it has only stable zeros. In this case, T^{-1} is stable and the solution K_{pre} can be easily obtained as $T^{-1}T_{ref}$. However, typical nanopositioning systems are flexure-based with non-collocated actuators and sensors, which typically manifest as non-minimum phase zeros of T. In this case, the optimal solution can be found by applying Nevanlinna-Pick theory [15] as follows.

The model-matching problem is equivalent to finding minimum γ such that $\|T_{ref}-TK_{pre}\|_\infty \leq \gamma$, where the

minimum $\gamma = \gamma_{opt}$ is achieved for some stable K_{pre}. If we define $E_\gamma = \frac{1}{\gamma}(T_{ref} - TK_{pre})$ for $\gamma > 0$, then our problem can be restated as finding a stable K_{pre} which requires $\|E_\gamma\|_\infty \leq 1$. Note that, for stable K_{pre}, E_γ satisfies the interpolating conditions $E_\gamma(z_i) = \frac{1}{\gamma}T_{ref}(z_i)$ for every non-minimum phase zero z_i of the closed-loop T. Therefore, we can cast this as a Nevanlinna-Pick (NP) problem - of finding a function E_γ in the space of stable, complex-rational functions such that it satisfies $\|E_\gamma\|_\infty \leq 1$ and $E_\gamma(z_i) = \frac{1}{\gamma}T_{ref}(z_i) \quad (i = 1, ..., n)$. Moreover, it can be shown that γ_{opt} is equal to the square root of the largest eigenvalue of the matrix $A^{-\frac{1}{2}}BA^{-\frac{1}{2}}$ where $A = [\frac{1}{z_i + \bar{z_j}}]$ and $B = [\frac{b_i \bar{b_j}}{z_i + \bar{z_j}}]$ [15]. The prefilter is given by $K_{pre} = T^{-1}(T_{ref} - \gamma_{opt}E_\gamma)$.

B. 2DOF Mixed Sensitivity Synthesis

In this control synthesis scheme, the regulated outputs were chosen to be the weighted tracking error $z_s = W_s e$, the weighted system output, $z_t = W_t y$, and the weighted control input, $z = W_u u$ to reflect the performance objectives and physical constraints (Figure 4).

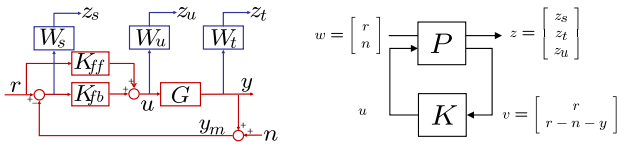

Fig. 4. Mixed sensitivity problem for 2DOF control design. The signals z_s, z_t, and z_u represent tracking error, the noise component in the position signal, and the control signal. The weights W_s, W_t and W_u are chosen to reflect the design specifications of tracking bandwidth, positioning resolution, and saturation limits on the control signal. To achieve these objectives, a control design $K = [K_{ff}\ K_{fb}]$ which minimizes the $\mathcal{H}_\infty$-norm of the transfer function from $w = [r\ n]$ to $z = [z_s\ z_t\ z_u]$ is sought through the optimal control problem.

However, 2 weight functions W_s and W_t are not enough to shape S_{er}, T_{ry}, S and T, thus we have included the weights W_r and W_n to reflect their frequency content as well as obtain greater independence in specifying trade-offs to the optimization problem. Using (2), the closed-loop matrix transfer function from w to z is given by

$$\begin{bmatrix} z_s \\ z_t \\ z_u \end{bmatrix} = \underbrace{\begin{bmatrix} W_s S_{er} W_r & -W_s S W_n \\ W_t T_{yr} W_r & -W_t T W_n \\ W_u S(K_{ff} + K_{fb}) W_r & -W_u S K_{fb} W_n \end{bmatrix}}_{=\Phi(K)} \begin{bmatrix} r \\ n \end{bmatrix}.$$

Accordingly, the $\mathcal{H}_\infty$ optimal control problem that we pose is $\min_K \|\Phi(K)\|_\infty$. The minimization of z_s reflects the tracking-bandwidth requirement. If we design W_s to be large in a frequency range of $[0\ \omega_{BW}]$ and ensure that z_s is small over the entire frequency range (through the above optimization problem) then the tracking-error e will be small in the frequency range $[0\ \omega_{BW}]$; that is the closed-loop positioning device has a bandwidth of ω_{BW}. Alternatively, note that the transfer function from r to z_s is $W_s S_{er} W_r$. The optimization problem along with our choice of W_s and W_r will ensure that the transfer function S_{er} is small in the frequency range $[0\ \omega_{BW}]$. Similarly, the transfer function from n to z_t is the weighted complementary sensitivity function $W_t T W_n$, whose minimization ensures better resolution as it forces low control gains at high frequencies, and the transfer function from r to z_u is $W_u S(K_{ff} + K_{fb}) W_r$, which measures the control effort. Its minimization reflects in imposing the practical limitation of the control signals to be within saturation limits.

IV. Experimental Implementation and Demonstration of Control Designs

This section demonstrates the optimal-control framework presented above on a two-dimensional flexure scanner of molecular force probe (MFP-3D) from Asylum Research Inc., Santa Barbara, CA.

A. Device Description

A schematic of the nanopositioning system (the scanner) is shown in Figure 5(a). It has two flexure components with component "X" stacked over the "Y" where the sample-holder is carried by the "X"-component. Each stage, by virtue of the serpentine spring design, deforms under the application of force, providing motion. These forces are generated by stack-piezos. The motion of each flexure component is measured by the corresponding nanopositioning sensors which is modified from linear variable differential transformer (LVDT) and the associated demodulation circuit. The piezoactuators yield a travel range of 90μm in close-loop in both directions. The sensors have noise less than 0.6nm (deviation) over 0.1 to 1kHz bandwidth. The control law is discretized and implemented on a Texas instrument TMS320C6713 digital signal processor(DSP) with 16bits A/D and 16bits D/A channels.

B. Identification

Physical modeling of the device is difficult due to its complicated structural design and poorly understood piezoactuation phenomena. Therefore, identification techniques were used to derive linear models about an operating point, where the sensor output gave a 'zero' reading corresponding to 'zero' input to the piezoactuators. The device is viewed as a two-input two-output system in which the low-voltage signals to the X and Y amplifiers are the inputs and the motion of X and Y flexure-stages components measured by the corresponding sensors, are the outputs. This results in four input-output transfer functions G_{ij}, i, j in $\{x, y\}$ (from input j to output i). The frequency-response based identification was done where a sine-sweep over a bandwidth from 1Hz-2kHz with amplitude 10mV was given to each axis using an HP 35670A signal analyzer. From the identification results, X and Y crosstalk represented by G_{xy} and G_{yx} are seen to be relatively small ($\|G_{xy}(j\omega)\|_\infty$ and $\|G_{xy}(j\omega)\|_\infty$ are less than -17.76dB), which is expected since, by design, X and Y flexure components are decoupled and are orthogonal to each other. Therefore, the nanopositioning system is modeled by two independent single input single output (SISO) units. The mode of operation of this device is such that higher bandwidth requirements are made on the smaller stage X, whereas the Y stage is made to move relatively slow. Hence,

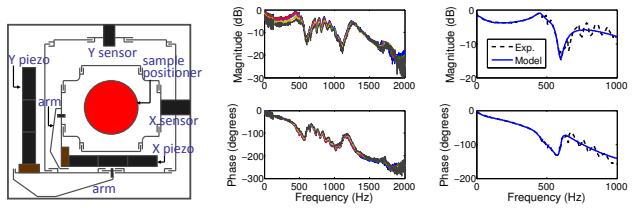

(a) (b) (c)

Fig. 5. (a) Schematic of flexure scanner: The sample is placed on the central block of the flexure stage which is driven by the x-piezo which in turn is driven by the y piezo. The x and y-sensors measure the current stage position. (b) Experimental frequency responses at various operating position. (c) Nominal frequency response(dashed) and model frequency response(solid).

there is a greater emphasis on the control designs for the X stage, which is presented in this paper.

This process was repeated to obtain frequency responses of the system at different operating points (by giving various DC offsets) spanning the range of operation of the device (Figure 5(b)). The variation in these responses is indicative of the modeling errors (uncertainties) in our identification scheme. In addition, it was observed that the frequency response at the same operating point varies when obtained at different times. In view of these uncertainties, robustness of the closed-loop system is a critical requirement of control design. The nominal frequency response of the system is obtained from averaging on 5 experiments on the nominal operating point which is of DC offset corresponds 0V at output. Figure 5(c) shows the bode diagram of fitted 7th order model with nominal experimental result. This 7th order model did not capture dynamics over 500Hz as shown in Figure 5(c). Its use is justified since the frequency range of interest is less than 500Hz and larger models result in implementations of higher order control which cannot be accommodated by the processor within short sampling time. This modeling uncertainty from using low order model was accounted for by imposing the requirement of making the closed-loop system robust to it on the control design.

C. Control designs, implementation and analysis

1) Optimal prefilter model matching: For the purpose of illustration, we designed a 9th order feedback "preexisting controller" by a feedback-only design based on $\mathcal{H}_\infty$ optimal framework which achieves much better bandwidth when compared to PI/PID designs [6]. Therefore, the improvements resulting on application of our model matching shown in this paper are even more substantial when applied to typical scanners that typically have PI/PID based feedback controllers. This feedback-only design yielded a bandwidth of 49.4 Hz, the roll-off frequency of 60.1 Hz, and $\|S\|_\infty$ of 1.15 for the closed-loop device (represented by dashed lines in Figure 6).

The prefilter is designed in pursuit of matching T as $T_{ref} = \frac{1}{0.0003s+1}$ by using the Nevanlinna-Pick (NP) solution. The control law from NP solution is improper and has relative order of degree -2, and therefore we multiplied by the weight function $W_0 = \frac{1.25}{(1\times10^{-4}s+1)^2}$ such that it becomes proper and has the same DC gain with T_{ref}.

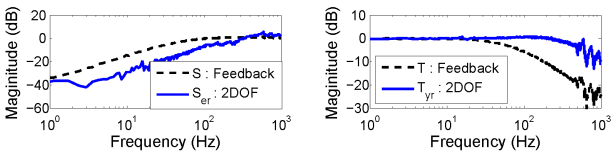

(a) (b)

Fig. 6. Comparison of experimentally obtained magnitude of $S(s)$ and $T(s)$ from $\mathcal{H}_\infty$ feedback-only control design with $S_{er}(s)$ and $T_{yr}(s)$ from 2DOF prefilter model matching control. The feedforward controller designed using prefilter model matching design achieves over 330% improvement in the tracking bandwidth of the closed-loop design. The robustness and resolution are determined by the feedback components S and T, and therefore remain the same for the two cases.

Figure 6 shows the experimentally obtained transfer function from reference to error i.e. S of feedback control and S_{er} of 2DOF control which represent the tracking performance (ω_{BW}=49.4Hz(feedback), =214.5Hz(2DOF)) (a) and the transfer function from reference to output i.e. T of feedback control and T_{yr} of 2DOF control (b). Thus this 2DOF design yields an improvement of over 330% in bandwidth over the feedback-only design. Since the feedback component of the two designs are the same and completely determines the robustness to modeling errors (characterized by $\|S\|_\infty$) as well as the positioning resolution (ω_T), the resolution and robustness remains the same for both the devices.

2) 2DOF mixed sensitivity synthesis: As discussed in section 3, four weight functions W_r, W_n, W_s, W_t are chosen to shape closed transfer functions: S_{er} with W_sW_r, S with W_sW_n , T_{yr} with W_tW_r, and T with W_tW_n. The performance objectives of high bandwidth, high resolution and robustness to modeling errors where reflected as follows. High resolution requires the roll-off frequency of ω_T to be small, that is T to be small beyond ω_T. This is imposed by designing the weight function $W_t = \frac{1000s+5.961\times10^4}{s+1.885\times10^5}$ to be large at high frequencies (we chose ω_t around 75 Hz). The range of frequencies where S is small (required for small tracking error) is restricted to small frequencies since small T at high frequencies implies S to be near 1 at high frequencies. Thus $W_s = \frac{0.3162s+3456}{s+3.456}$ ensures S is small at low frequencies and allows for its cross-over frequency to be small enough to make designed ω_T feasible. Figure 7(a,b) shows the choice of the weight functions that reflect these objectives. The choice of W_r and W_n is made such that at the frequency the W_t starts increasing, W_r starts increasing and W_n starts decreasing (in fact W_n is chosen as inverse of W_r). Note that at the frequency where W_s stop rolls off, W_r and W_n converge to 1. This choice of W_r and W_n ensures that S_{er} is small even when S is not small. This is done by exploiting that S is shaped by W_s while S_{er} is shaped by W_sW_r. The choice of weight function $W_u = 0.1$ restricted control signal values to be within saturation limits.

The feedforward and feedback control laws obtained from $\mathcal{H}_\infty$ mixed sensitivity synthesis procedure were implemented. Figure 7(c,d) shows the experimentally obtained transfer function from reference to error i.e. $S_{er}(s)$ which represents the tracking performance (ω_{BW}= 148.2Hz) in (c)

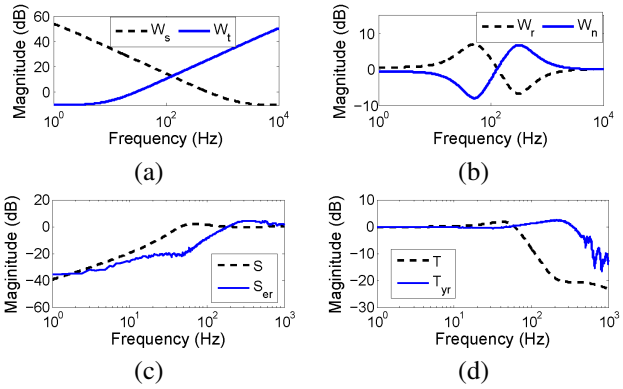

Fig. 7. (a,b) Choice of weight functions. (c,d) Magnitude of $S_{er}(s)$ and $T_{yr}(s)$(solid) obtained from experiment and S and T(dashed) obtained from simulation

and the transfer function from reference to output i.e. $T_{yr}(s)$ in (d). There was in improvement of 290% in bandwidth for same values of resolution and robustness if compared to feedback-only design.

V. Analysis and Discussion

(I) Relative roles of feedforward and feedback: Noting that $S_{er} = S(1 - GK_{ff})$, and S cannot be made small over the entire bandwidth range (in order to allow for noise attenuation), the feedforward control is 'active' in making S_{er} small beyond the frequency where $|S|$ is not small (say greater than $1/\sqrt{2}$). Also since $S = (1 + GK_{fb})^{-1}$ is completely determined by K_{fb}, the feedback component is dominant in frequencies where S is small. Therefore the main contribution of feedforward component is in the frequency range where S is no longer small. However this frequency range is limited. Typically nanopositioning systems have very low gains beyond their flexure resonance frequencies. Therefore very high control inputs are needed to make the positioning systems practical beyond their flexure resonances. The saturation limits on control signals form the main constraints on attaining bandwidths beyond flexure resonances. Thus the feedforward components provide performance *enhancements* over feedback-only designs in the frequency range from corner frequency of S to the flexure resonance frequency. This perspective is further justified from the fact that the 2DOF mixed sensitivity optimal control designs, where the optimization problem does not discriminate between feedforward and feedback components with respect to performance objectives, exhibit this separation of their roles.

(II) Breaking barriers of feedback-only design: The 2DOF design is not bound by some fundamental limitations that constrain the feedback-only designs. For instance the results in Section IV show that in 2DOF design, the tracking bandwidth ω_{BW} of the closed-loop device can be made larger than the roll off frequency ω_T which determines the resolution. The corner frequency ω_{BW} can *never* be made larger than ω_T in feedback-only design, which suffers from a stricter trade-off between the resolution and the bandwidth. For 2DOF prefilter model matching control based on $\mathcal{H}_\infty$ controller has ω_{BW} of 214.5Hz and ω_T of 60.1Hz while original $\mathcal{H}_\infty$ controller has the bandwidth of 49.4Hz and the same roll-off frequency. This example gives a case where 2DOF design achieves specifications that are *impossible* to attain with feedback-only design.

(III) Control-design extensions: The 2DOF designs presented here can be easily extended to achieve a larger class of design specifications than presented in this paper with trivial or no modifications to the designs presented here. For instance, we have not exploited the frequency content of the reference signals into our design. This can be easily incorporated by writing the reference signal as $r = H(j\omega)r'$, where r' is arbitrary signal (as used in our analysis) and the transfer function $H(j\omega)$ reflects the frequency content of the signal. Alternatively we can incorporate the frequency content of the reference signal through the model transfer functions T_{ref} or through weight transfer functions.

References

[1] R. Koops and G. Sawatzky, "New scanning device for scanning tunneling microscope applications," *Review of Scientific Instruments*, vol. 63, no. 8, pp. 4008–9, August 1992.

[2] H. Kaizuka, "Application of capacitor insertion method to scanning tunneling microscopes," *Review of Scientific Instruments*, vol. 60, no. 10, pp. 3119–3122, 1989.

[3] D. Croft, G. Shedd, and S. Devasia, "Creep, hysteresis and vibration compensation for piezoactuators: Atomic force microscopy application," *Journal of Dynamic Systems, Measurement and Control*, vol. 123, pp. 35–43, 2001.

[4] A. G. Hatch, R. C. Smith, T. De, and M. V. Salapaka, "Construction and experimental implementation of a model-based inverse filter to attenuate hysteresis in ferroelectric transducers," *IEEE Transactions on Control Systems Technology*, vol. 14, no. 6, pp. 1058 – 1069, 2006.

[5] K. Leang and S. Devasia, "Hysteresis, creep and vibration compensation for piezoactuators: feedback and feedforward control," in *Proceedings of 2nd IFAC Conference on Mechatronic Systems*, 2002, pp. 283–289.

[6] S. Salapaka, A. Sebastian, J. P. Cleveland, and M. V. Salapaka, "High bandwidth nano-positioner: A robust control approach," *Review of Scientific Instruments*, vol. 73, no. 9, pp. 3232–3241, 2002.

[7] G. Schitter, P. Menold, H. F. Knapp, F. Allgower, and A. Stemmer, "High performance feedback for fast scanning atomic force microscopes," *Review of Scientific Instruments*, vol. 72, no. 8, pp. 3320–3327, August 2001.

[8] A. Sebastian and S. Salapaka, "Design methodologies for robust nano-positioning," *IEEE Transactions on Control Systems Technology*, vol. 13, no. 6, pp. 868–876, 2005.

[9] G. Schitter, F. Allgower, and A. Stemmer, "A new control strategy for high speed atomic force microscopy," *Nanotechnology*, vol. 15, no. 1, pp. 108–114, 2004.

[10] Y. Wu and Q. Zou, "Iterative control approach to compensate for both the hysteresis and the dynamics effects of piezo actuators," *IEEE Transaction on Control Systems Technology*, vol. 15(5), pp. 936–944, September 2007.

[11] B. E. Helfrich, C. Lee, D. A. Bristow, X. Xiaohui, J. Dong, A. G. Alleyne, and S. Salapaka, "Combined $\mathcal{H}_\infty$-feedback and iterative learning control design with application to nanopositioning systems," in *Proceedings of American Control Conference, Seattle, WA*, June 2008, pp. 3893– 3900.

[12] S. Skogestad and I. Postlethwaite, *Multivariable Feedback Control, Analysis and Design*, 2nd ed. John Wiley and Sons, 2005.

[13] J. S. Freudenberg and D. P. Looze, "Right half-plane poles and zeros and design tradeoffs in feedback systems," *IEEE Transactions on Automatic Control*, vol. 30, no. 6, pp. 555–565, 1985.

[14] C. Mohtadi, "Bode's integral theorem for discrete-time systems," *Control Theory and Applications, IEE Proceedings D*, vol. 137, pp. 57–66, 1990.

[15] J. C. Doyle, B. A. Francis, and A. R. Tannenbaum, *Feedback control theory*. New York: MacMillan, 1992.